symmetry

IMPACT FACTOR 2.2

CITESCORE 5.3

Article

Canonical Effect on Quarkonium Enhancement in the Deconfined Medium

Aidan Zhou, Shiqi Zheng and Baoyi Chen

MDPI

https://doi.org/10.3390/sym17060830

symmetry

MDPI

Article

Canonical Effect on Quarkonium Enhancement in the Deconfined Medium

Aidan Zhou [1], Shiqi Zheng [2,*] and Baoyi Chen [3,*]

[1] International School of Beijing, Beijing 101318, China
[2] Department of Civil Engineering and Engineering Mechanics, Columbia University, New York, NY 10027, USA
[3] Department of Physics, Tianjin University, Tianjin 300350, China
* Correspondence: sz3357@columbia.edu (S.Z.); baoyi.chen@tju.edu.cn (B.C.)

Abstract: Studying strong interactions at finite temperatures has been a critical topic in high-energy nuclear collisions. Charmonium, as a clear probe of deconfined matter, is believed to be predominantly influenced by the coalescence of off-diagonal charm and anti-charm quarks. The grand canonical ensemble is commonly used to describe the coalescence of charm and anti-charm quarks. In collisions where only one or two charm pairs are produced, the contribution from the coalescence of diagonal charm and anti-charm quarks becomes dominant, a phenomenon known as the canonical effect. This effect is sensitive to the momentum correlation between the heavy quark and anti-quark. In this work, we employ the Langevin model to study the evolutions of correlated charm and anti-charm quarks and their coalescence process. The asymmetry in the momentum of charm and anti-charm quarks play important roles in their coalescence process. In addition, we investigate the impact of this effect on the nuclear modification factor of charmonium, which can be enhanced evidently in semi-central collisions at RHIC Au-Au collisions. The theoretical calculations with canonical effect explain the experimental data well, which helps us to understand the production mechanisms of the quarkonium bound state in the deconfined medium.

Keywords: high energy physics; quark-gluon plasma; heavy quark; langevin equation

Academic Editor: Stefano Profumo

Received: 1 May 2025
Revised: 19 May 2025
Accepted: 21 May 2025
Published: 26 May 2025

Citation: Zhou, A.; Zheng, S.; Chen, B. Canonical Effect on Quarkonium Enhancement in the Deconfined Medium. *Symmetry* **2025**, *17*, 830. https://doi.org/10.3390/sym17060830

1. Introduction

It has been widely accepted that the early universe, shortly after the Big Bang, consisted of partons with extremely high energy densities. This state of matter, known as Quark–Gluon Plasma (QGP), can be recreated on Earth through collisions between heavy nuclei at relativistic speeds, such as those occurring in the Relativistic Heavy-Ion Collider (RHIC) [1] and the Large Hadron Collider (LHC) [2]. In these experiments, the kinetic energy of colliding nuclei is converted into particles and anti-particles in the collision zone, leading to the formation of deconfined matter [3]. Understanding the properties of this deconfined matter, including its coupling strength [4] and viscosity [5], is crucial for both the Standard Model and the mechanisms of particle production. Such studies also contribute to the exploration of strong interactions at high temperatures and baryon densities.

Over the past forty years, numerous physical observables have been proposed to study the properties of hot QCD matter [6–9]. Unlike light partons, which can be easily thermally produced due to their small masses, the large mass of heavy quarks prevents their thermal production in the QGP. Instead, heavy quarks are primarily produced in the initial hard scatterings of partons at the beginning of nuclear collisions. Moreover, the

dynamical evolution of heavy quarks can be effectively described using the transport and statistical models [10–13]. These characteristics make heavy-flavor particles ideal probes of QGP. For heavy quarkonium, which consists of a heavy quark and an anti-quark, the binding energies can be reduced by the hot medium, making them an ideal "thermometer" in heavy-ion collisions. In such collisions, quarkonium is more easily dissociated in the hotter medium.

At LHC collision energies, a hotter QCD matter is expected. Experimental data indicate a weaker suppression of charmonium yield in this hotter QGP. This yield enhancement is attributed to the coalescence of charm and anti-charm quarks. In the QGP, the coalescence probability between charm and anti-charm quarks increases significantly, and the yield of regenerated charmonium is proportional to the product of the number of charm and anti-charm quarks, i.e., $\propto (N_{c\bar{c}})^2$ [14]. Most charm and anti-charm quarks originate from different pairs, a phenomenon referred to as off-diagonal elements in the charmonium regeneration matrix [15]. This coalescence follows the grand canonical ensemble when $N_{c\bar{c}}$ is large.

However, in nuclear collisions at RHIC energies or in small collision systems like proton–nucleus (p-Pb) or high-multiplicity proton–proton (pp) collisions, only one or two charm pairs are produced in each collision event. The coalescence probability between off-diagonal charm and anti-charm quarks is suppressed due to the small number of charm pairs in the small QGP. In a $c\bar{c}$ pair, since charm and anti-charm quarks are produced simultaneously and nearly at the same spatial coordinate, their coalescence probability may play a more significant role compared to the contribution of off-diagonal charm and anti-charm quarks. In this scenario, the yield of charmonium from coalescence is proportional to the number of charm pairs, i.e., $\propto (N_{c\bar{c}})$, and satisfies the canonical ensemble [16–20]. This canonical effect becomes more dominant in the case of bottom quarks and bottomonium, where the number of bottom pairs becomes smaller [21]. Most theoretical models employ the grand canonical ensemble to study charmonium coalescence and neglect the momentum correlation between c and $\bar{c}$ quarks. In this work, we will examine the momentum correlation of $c\bar{c}$ and its effects on the coalescence of charmonium at RHIC energies, which is crucial for understanding the experimental data of charmonium nuclear modification factor.

We use the Langevin equation to describe the dynamical evolutions of a pair of heavy quarks simultaneously, calculate their angular correlation, and determine the probability of their recombination into a charmonium bound state in the QGP. In Section 2, the details of the Langevin model are introduced. In Section 3, we present numerical calculations of the angular correlation between charm and anti-charm quarks when they move out of QGP, as well as the regeneration probability of the correlated charm and anti-charm quarks into quarkonium. We also compare the theoretical calculations with the experimental data. Finally, in Section 4, a summary is provided.

2. Theoretical Model

2.1. Heavy Quark Dynamics and Coalescence

Due to the large mass of heavy quarks, their dynamical evolution in the medium can be described by a classical equation. Previous studies have shown that the momentum evolution of heavy quarks is well captured by the Langevin equation [9,22–24]. The effects of random scatterings between heavy quark and thermal particles are parametrized through the drag and noise terms in the Langevin equation:

$$\frac{d\mathbf{p}}{dt} = -a(p)\mathbf{p} + \mathbf{b}(t) \quad (1)$$

where $\mathbf{p}$ denotes the vector of the heavy quark momentum. The parameters $a(p)$ and $\mathbf{b}(t)$ correspond to the drag and random noise terms, respectively. The drag term is defined as $a(p) = \kappa/(2TE_Q)$, where T is the medium temperature and $E_Q = \sqrt{m_c^2 + p^2}$ is the heavy quark energy with the mass $m_c = 1.5$ GeV. The parameter $\kappa = 2T^2/D_s$, where D_s is the spatial diffusion coefficient. Extensive studies on the diffusion coefficient have been conducted, and its value is taken as $D_s 2\pi T = 2.0$ according to previous work [25]. The white noise term $\mathbf{b}(t)$ satisfies the relation $\langle b^i(t) b^j(t') \rangle = \kappa \delta_{ij} \delta(t - t')$, where i, j represent the indices of the three dimensions.

The initial distribution of heavy quarks is proportional to the density of binary collisions. Due to Lorentz contraction, the initial density of charm quarks in the transverse plane can be expressed as

$$\frac{dN_{c\bar{c}}}{dyd\mathbf{x}_T} = \frac{d\sigma_{c\bar{c}}^{pp}}{dy} T_A(\mathbf{x}_T - \mathbf{b}/2) T_B(\mathbf{x}_T + \mathbf{b}/2), \tag{2}$$

where $\mathbf{x}_T$ is the transverse plane, with longitudinal direction defined to be the nuclear acceleration direction. $\mathbf{b}$ is the impact parameter, defined to be the distance between the centers of two nuclei when they collide with each other. $T_A(\mathbf{x}_T) = \int dz \rho(\mathbf{r})$ is the thickness function which characterizes the nucleon density on the transverse plane. The nucleon density $\rho(\mathbf{r})$ is taken as the Woods–Saxon distribution. The charm production cross section as a function of rapidity y has been measured by experiments, which will be given below. The initial momentum of heavy quarks is generated by the PYTHIA. With the initial distributions of charm quarks, one can randomly generate the initial position and momentum of each charm and anti-charm quark event-by-event, and evolve them respectively with the Langevin equation.

The temperatures and velocities of the bulk medium are also required in the Langevin equation. Since the deconfined medium is found to behave like a nearly perfect fluid, which can be well described with a hydrodynamic model, we employ the MUSIC package to generate the temperature and velocity profiles of the medium [26,27]. The initial energy density profiles, which serve as input for the hydrodynamic model, are generated using the Glauber model [28]. Given that the number of charm pairs is small in RHIC 200 GeV Au-Au collisions and in smaller collision systems such as pp and p-Pb collisions, we consider the momentum correlations of diagonal charm and anti-charm quarks produced in the same partonic hard scattering and their subsequent coalescence into charmonium within the framework of the canonical ensemble. The momentum correlation between diagonal charm and anti-charm quarks not only serves as a valuable observable to quantify the effects of QGP, but is also crucial for the enhancement of charmonium production. Hot QCD matter interacts with heavy quarks through random scatterings, causing their momentum to become decoherent [29]. The momentum correlation between c and $\bar{c}$ after they exit the hot QCD medium is defined as

$$\cos\theta = \frac{\mathbf{p}_c \cdot \mathbf{p}_{\bar{c}}}{|\mathbf{p}_c| \cdot |\mathbf{p}_{\bar{c}}|}. \tag{3}$$

Hot medium effects are encoded in the angle θ between the final momenta of the two heavy quarks. The initial momenta of most diagonal charm and anti-charm quarks are close to back-to-back correlation. As the quarks propagate through the thermal medium, random interactions with the bulk medium modify their relative momentum, resulting in a change in the corresponding angle θ. These will be calculated in the next section.

When the relative momentum and distance between the charm and anti-charm quarks become sufficiently small, they can combine to form a charmonium bound state via the reaction $c + \bar{c} \to J/\psi + g$ in regions of the medium with low temperature. The coalescence

probability is determined by the Wigner function, which is related to the wave function of the resulting hadrons. The Wigner function $W(\mathbf{x}_r, \mathbf{p}_r)$ can be approximated as a Gaussian function [30]:

$$W(\mathbf{x}_r, \mathbf{p}_r) = 8 \exp(-\frac{x_r^2}{\sigma^2}) \exp(-p_r^2 \sigma^2), \tag{4}$$

where $\mathbf{x}_r = \mathbf{x}_c^{cm} - \mathbf{x}_{\bar{c}}^{cm}$ and $\mathbf{p}_r = \frac{E_c^{cm}\mathbf{p}_{\bar{c}}^{cm} - E_{\bar{c}}^{cm}\mathbf{p}_c^{cm}}{E_c^{cm} + E_{\bar{c}}^{cm}}$ represent the relative position and relative momentum in the center-of-mass frame of the charm and anti-charm quarks, respectively. The width of the Wigner function is related to the root-mean-square radius of the formed state, given by $\sigma^2 = \frac{8}{3}\langle r^2 \rangle_M$ [31]. For the ground state of charmonium, the value $\sqrt{\langle r^2 \rangle_{J/\psi}} = 0.5$ fm is used, based on studies with the potential model [14].

According to the in-medium properties of charmonium, the coalescence process happens in the medium with the local temperature $T_{\rm coal}$ to be close to the critical temperature [32]. By utilizing the distribution of heavy quarks in phase space and their coalescence probabilities, one can calculate the production of charmonium through coalescence [23,33] and investigate the modification of the canonical effect:

$$\frac{dN}{d\mathbf{p}_\psi d\mathbf{x}_\psi} = \int \frac{d\mathbf{p}_c d\mathbf{x}_c}{(2\pi)^3} \frac{d\mathbf{p}_{\bar{c}} d\mathbf{x}_{\bar{c}}}{(2\pi)^3} f(\mathbf{x}_c, \mathbf{p}_c, \mathbf{x}_{\bar{c}}, \mathbf{p}_{\bar{c}}) W(\mathbf{x}_r, \mathbf{p}_r) \times \delta(\mathbf{p}_\psi - \mathbf{p}_c - \mathbf{p}_{\bar{c}}) \delta(\mathbf{x}_\psi - \frac{\mathbf{x}_c + \mathbf{x}_{\bar{c}}}{2}). \tag{5}$$

In the grand canonical ensemble, the distributions of charm and anti-charm quarks are independent of each other, such that $f(\mathbf{x}_c, \mathbf{p}_c, \mathbf{x}_{\bar{c}}, \mathbf{p}_{\bar{c}}) = f_c(\mathbf{x}_c, \mathbf{p}_c) f_{\bar{c}}(\mathbf{x}_{\bar{c}}, \mathbf{p}_{\bar{c}})$. In this case, the distribution of $dN/d\mathbf{p}_\psi$ is proportional to the square of the charm number, $\propto (N_{c\bar{c}})^2$. However, in the canonical ensemble, the charmonium yield becomes proportional to $N_{c\bar{c}}$. The canonical effect can enhance the charmonium yield when the number of charm pairs is expected to be smaller than one in heavy-ion collisions. There are two key differences between the grand canonical and canonical ensembles in this model: the yield correlation and the momentum correlation between charm and anti-charm quarks. In the case of the canonical ensemble, a constraint requires that an anti-charm quark must be produced whenever a charm quark is produced. This means that charmonium production depends on $\sigma_{pp}^{c\bar{c}}$, rather than the square $(\sigma_{pp}^{c\bar{c}})^2$ as previously mentioned. This difference can significantly enhance charmonium production, particularly when the charm pair production cross section is small. Another important factor is that in the canonical ensemble, charm and anti-charm quarks are produced at the same position with correlated momenta. This can also increase their coalescence during the evolution. These correlations in both yield and momentum distribution are not taken into account in the grand canonical ensemble case.

2.2. Quarkonium Primordial Production

Quarkonium can also be produced in the initial partonic hard scatterings. Due to the large binding energies of J/ψ, their dissociation temperatures are above the critical temperature, T_c, of the phase transition. Some of the charmonium produced primordially can survive in the hot QCD medium, particularly in semi-central and peripheral collisions, where the energy densities of the bulk medium are not excessively high. The suppression of primordial charmonium production in the hot medium can be effectively described by the transport equation [34,35]:

$$\partial_t f_\psi + \mathbf{v} \cdot \bigtriangledown_{\mathbf{x}} f_\psi = -\alpha_\psi f_\psi \tag{6}$$

where f_ψ is the distribution of charmonium in phase space, and $\mathbf{v}$ is the velocity. The term involving $\mathbf{v}$ represents the diffusion of charmonium in the medium with a constant velocity. α_ψ is the decay rate of charmonium, which reduces the distribution f_ψ. It is written as

$$\alpha_\psi = \frac{1}{2E_T}\int \frac{d^3\mathbf{k}}{(2\pi)^3 2E_g}\sigma_{g\Psi}(\mathbf{p},\mathbf{k},T)4F_{g\Psi}(\mathbf{p},\mathbf{k})f_g(\mathbf{k},T) \tag{7}$$

Here, E_T is the transverse energy of charmonium, while $\mathbf{k}$ and E_g represent the momentum and energy of the gluon, respectively. The thermal distribution of the gluon is taken as the Bose distribution. The inelastic scattering cross section between charmonium and the gluon is calculated in previous references [34,36]. A color-screened binding energy of J/ψ is employed in the collision cross section. The decay rate of the J/ψ at different temperatures is plotted in the figure below. For the excited states ($\chi_c, \psi(2S)$), their decay rates can be obtained through a geometric scaling with the ground state [35]. The decay width of charmonium eigenstates (1S, 1P, 2S) as a function of temperature are plotted in Figure 1. It is consistent with other models [37,38].

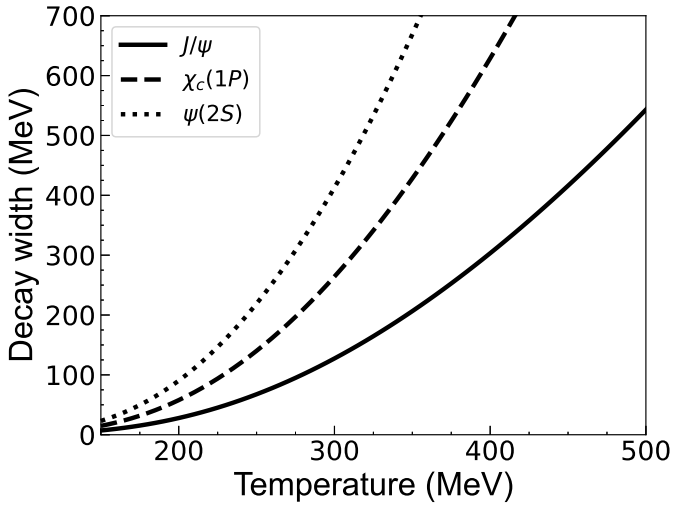

Figure 1. The decay width of charmonium states (1S, 1P, 2S) as a function of the medium temperature.

To solve the transport equation, the initial distribution of charmonium is also needed as an input. The initial momentum distribution of charmonium has been parametrized [39] based on experimental measurements in pp collisions. The charmonium production in nucleus–nucleus collisions can be treated as a superposition of pp collisions. Therefore, the initial spatial distribution of charmonium in a given rapidity bin can be obtained as $f_\psi(\mathbf{x}, \tau = 0) = \frac{d\sigma_{pp}^{J/\psi}}{dy} T_A(\mathbf{x} - \mathbf{b}/2) T_B(\mathbf{x}_T + \mathbf{b}/2)$. The rapidity differential cross section is written as $\frac{d\sigma_{pp}^{J/\psi}}{dy} = 2$ μb for central rapidity pp collisions at $\sqrt{s_{NN}} = 200$ GeV according to Pythia simulations [40].

3. Numerical Results in Heavy-Ion Collisions

The hot deconfined medium dissociates heavy quarkonium and suppresses its yield due to the color screening effect and parton inelastic scatterings [41,42]. At the same time, the deconfined medium provides an environment in which heavy quarks and anti-quarks can diffuse and combine into new quarkonium. This regeneration occurs when the in-medium heavy quark potential is restored at low temperatures, allowing the bound states to survive in the medium. Experimental and theoretical studies have shown that regeneration plays a significant role in nuclear collisions at RHIC energies. In the grand canonical ensemble, it is assumed that charm and anti-charm quarks participating in the coalescence

are produced in different initial parton hard scatterings, with their initial positions and momenta being uncorrelated. However, in nuclear collisions at RHIC energy, the number of heavy quarks in a given rapidity bin is small, suggesting that the canonical ensemble should be used instead.

In Figure 2, the number of charm quark pairs per rapidity is shown as a function of the impact parameter b. The production cross section for charm pairs is taken as $d\sigma_{pp}^{c\bar{c}}/dy = 120$ µb [43] in the central rapidity region of 200 GeV proton–proton collisions. As shown in the figure, the number of charm pairs is approximately 3.5 in the most central Au-Au collisions within a unit rapidity and decreases to less than 2 in semi-central collisions. This indicates that the coalescence of charm and anti-charm quarks should occur within the same pair, and the correlation between their positions and momenta must be taken into account. The relative position and relative momentum between the charm and anti-charm quarks are crucial factors for determining their coalescence probability.

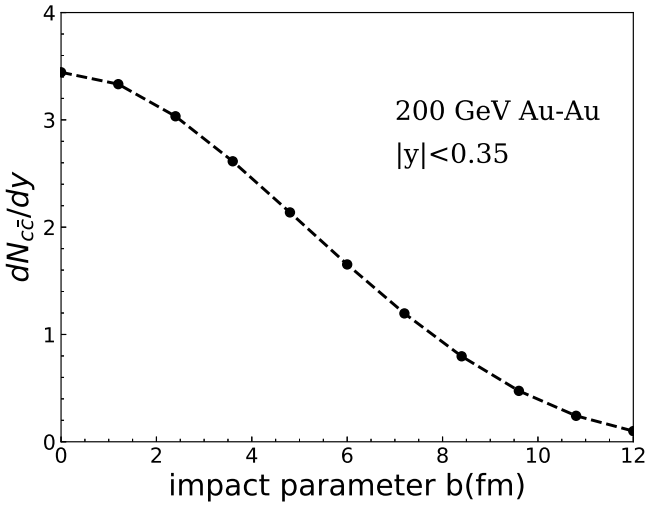

Figure 2. The number of charm pairs per rapidity as a function of the impact parameter b in 200 GeV Au-Au collisions.

The momentum correlation is considered and plotted in Figure 3. In the upper panel, heavy quarks from the entire p_T region are considered. The angle distribution of the initial momenta of charm and anti-charm quarks is plotted with a thin black dashed line. As the heavy quarks move out of the hot QCD medium, the angle distribution between their final momenta is shown with thick lines in Figure 3. Different bulk media are considered by taking the impact parameter to be $b = 0$ (central collisions) and $b = 8.4$ fm (semi-central collisions), respectively. As shown in the figure, the initial back-to-back correlation between heavy quarks' momenta is washed out by the hot medium due to random collisions with thermal particles, as seen in the thick red line. The spatial diffusion coefficient, which characterizes the coupling strength between heavy quarks and the medium, is taken as $D_s 2\pi T = 2$. To better illustrate the medium effects on heavy quarks with different momenta, the lower panel of Figure 3 shows the initial momenta of the charm quarks selected to be $p_T > 1$ GeV/c. Due to the higher initial momenta of the charm quarks, their motion is less affected by random collisions in the thermal medium. As a result, after the heavy quark evolution, their angular correlation retains part of its initial structure.

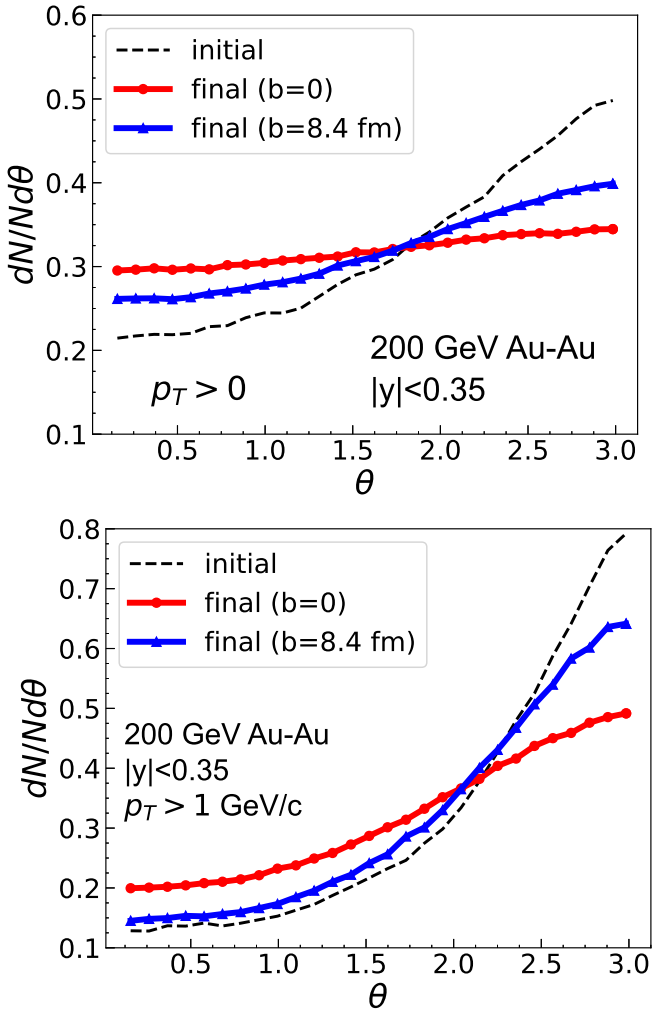

Figure 3. (**Upper panel**) The angle distribution between the momenta of charm and anti-charm quarks in 200 GeV Au-Au collisions. The transverse momentum of heavy quarks is selected to be $p_T > 0$. The thin dashed line is for their initial momentum. The thick red and thick blue lines are for the final angle correlation between charm and anti-charm quarks in central (b = 0) and semi-central (b = 8.4 fm) collisions, respectively. The spatial diffusion coefficient in the Langevin equation is taken to be $D_s 2\pi T = 2.0$. (**Lower panel**) Same as the upper panel except that the momentum of charm quarks is selected in $p_T > 1$ GeV/c to show the correlation of charm quarks in a higher p_T region.

In the calculation of charmonium regeneration from diagonal charm pairs, it is essential to exclude primordial production and focus on the effects of the hot medium on charmonium regeneration. Since the typical formation time for primordially produced charmonium ground states is approximately $t_{\rm form} = 0.6$ fm/c [44], we assume that the regeneration process occurs only for $t > t_{\rm form}$. The coalescence process takes place when charm quarks move to the edge of the hot QCD medium. In the grand canonical ensemble, the initial positions and momenta of c and $\bar{c}$ quarks are independent of each other. In the canonical ensemble, however, the c and $\bar{c}$ quarks involved in coalescence originate from the same position, and the angle between their initial momenta follows the correlation described above. As shown in Figure 4, charmonium regeneration is approximately 1.2 times greater in the canonical ensemble compared to the grand canonical ensemble. This enhancement becomes more pronounced in semi-central and peripheral collisions, where fewer charm pairs are produced, as illustrated in the lower panel of Figure 4.

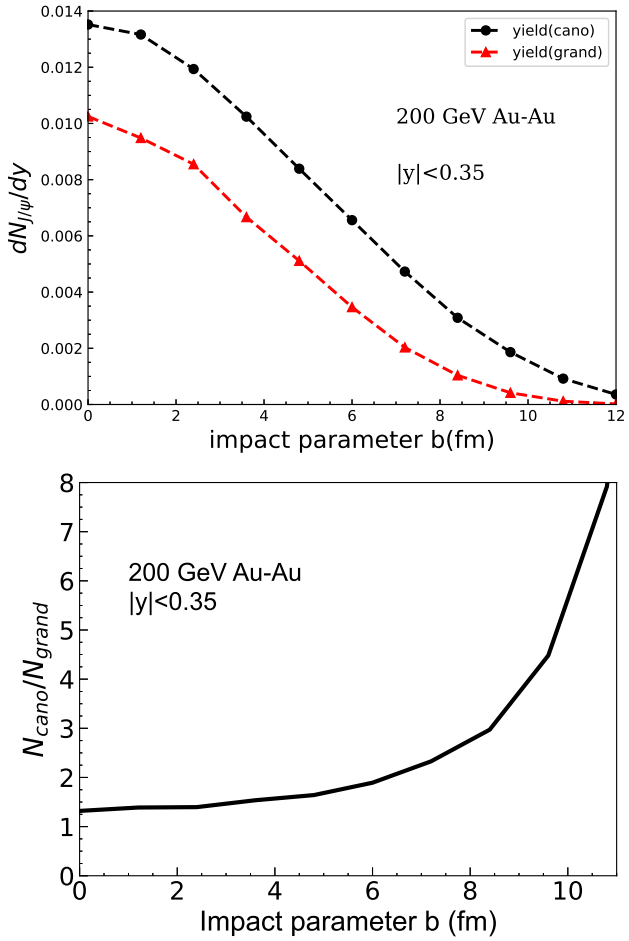

Figure 4. (**Upper panel**) Charmonium regeneration as a function of the impact parameter in 200 GeV Au-Au collisions is shown. The black line with circle markers represents the canonical ensemble, accounting for correlations between charm and anti-charm quarks. The red line with triangle markers corresponds to the grand canonical ensemble. (**Lower panel**) The ratio of charmonium regeneration in the canonical and grand canonical ensembles.

To better illustrate the effect of the canonical ensemble on the physical observable, we also calculate the charmonium nuclear modification factor, R_{AA}, defined as follows:

$$R_{AA} = \frac{N^{\psi}_{AA}}{N^{\psi}_{pp,ncoll}}, \tag{8}$$

where $N^{\psi}_{pp,ncoll}$ is the charmonium production in pp collisions scaled by the number of binary collisions. It represents charmonium production without the effects of hot QCD matter in nuclear collisions. In the numerator, N^{ψ}_{AA} includes both primordial production at the beginning of the medium evolution (formed at $t < t_{\rm form}$) and production from coalescence in the later stage (formed at $t > t_{\rm form}$). In Figure 5, the primordial production is plotted with the dotted line. The regeneration from canonical ensemble and grand canonical ensemble are plotted with the thick black dashed line and thin red dashed line, respectively. The prompt R_{AA} is plotted with solid lines: thick solid lines consider the correlations of diagonal charm and anti-charm quarks, while the thin red line does not. As one can see, the canonical ensemble effect can enhance the regeneration and make the prompt R_{AA} explain the experimental data well. This behavior also helps explain the experimental data of charmonium R_{AA} in semi-central Pb-Pb collisions at 5.02 TeV [45]. When considering

the canonical ensemble, the regeneration of R_{AA} is enhanced. The trend of the regenerated R_{AA} with N_p is consistent with other theoretical models [37]. Therefore, it is necessary to include the canonical ensemble in the interpretation of the experimental data.

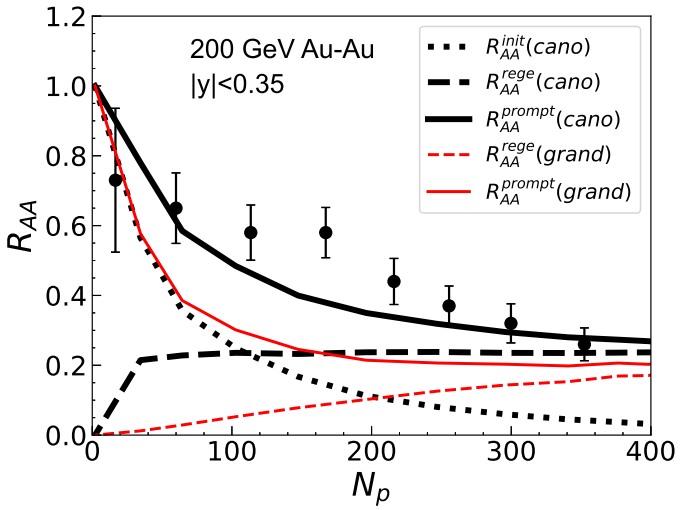

Figure 5. The charmonium nuclear modification factor R_{AA} as a function of the number of participants in 200 GeV Au-Au collisions is shown. Prompt, primordial, and regenerated yields are plotted with the solid, dotted, and dashed lines, respectively. Thick lines are for the canonical ensemble, while the thin lines are for the grand canonical ensemble. The experimental data are cited from [46].

4. Summary

This work studies the momentum correlation between diagonal charm and anti-charm quarks and their coalescence into charmonium. In nuclear collisions at RHIC energy, the charm pair number is relatively small, making the grand canonical ensemble unsuitable for calculating charmonium regeneration. Instead, the charm and anti-charm quarks produced in the same reaction can combine to form charmonium during their evolution in the medium. The energy loss of heavy quarks is described using the Langevin equation, while the hadronization process is modeled using the coalescence model. Our calculations explain well the experimental data of charmonium at RHIC energies, suggesting that the canonical ensemble effect is important at RHIC energies and dominates charmonium regeneration. Thus, studying the momentum correlation between diagonal charm and anti-charm quarks helps to understand charmonium regeneration and offers insights into detecting the deconfined medium in nuclear collisions.

Author Contributions: Conceptualization, A.Z. and S.Z.; methodology, A.Z. and S.Z.; software, A.Z. and S.Z.; validation, S.Z.; formal analysis, B.C.; investigation, A.Z. and B.C.; resources, B.C.; data curation, A.Z.; writing—original draft preparation, A.Z.; writing—review and editing, B.C.; visualization, B.C.; supervision, B.C.; project administration, B.C.; funding acquisition, B.C. All authors have read and agreed to the published version of the manuscript.

Funding: This research was supported by the National Natural Science Foundation of China (NSFC), Grant Number 12175165.

Data Availability Statement: Data are contained within the article.

Conflicts of Interest: The authors declare no conflicts of interest.

References

1. Adams, J.; Aggarwal, M.M.; Ahammed, Z.; Amonett, J.; Anderson, B.D.; Arkhipkin, D.; Averichev, G.S.; Badyal, S.K.; Bai, Y.; Balewski, J.; et al. Experimental and theoretical challenges in the search for the quark gluon plasma: The STAR Collaboration's critical assessment of the evidence from RHIC collisions. *Nucl. Phys. A* **2005**, *757*, 102–183. [CrossRef]
2. Gyulassy, M.; McLerran, L. New forms of QCD matter discovered at RHIC. *Nucl. Phys. A* **2005**, *750*, 30–63. [CrossRef]
3. Bazavov, A.; Bhattacharya, T.; Cheng, M.; DeTar, C.; Ding, H.T.; Gottlieb, S.; Gupta, R.; Hegde, P.; Heller, U.M.; Karsch, F.; et al. The chiral and deconfinement aspects of the QCD transition. *Phys. Rev. D* **2012**, *85*, 054503. [CrossRef]
4. Song, H.; Bass, S.A.; Heinz, U.; Hirano, T.; Shen, C. 200 A GeV Au+Au collisions serve a nearly perfect quark-gluon liquid. *Phys. Rev. Lett.* **2011**, *106*, 192301; Erratum in *Phys. Rev. Lett.* **2012**, *109*, 139904. [CrossRef]
5. Heinz, U.; Snellings, R. Collective flow and viscosity in relativistic heavy-ion collisions. *Ann. Rev. Nucl. Part. Sci.* **2013**, *63*, 123–151. [CrossRef]
6. Alver, B.; Roland, G. Collision geometry fluctuations and triangular flow in heavy-ion collisions. *Phys. Rev. C* **2010**, *81*, 054905; Erratum in *Phys. Rev. C* **2010**, *82*, 039903. [CrossRef]
7. Qin, G.Y.; Wang, X.N. Jet quenching in high-energy heavy-ion collisions. *Int. J. Mod. Phys. E* **2015**, *24*, 1530014. [CrossRef]
8. Pang, L.; Wang, Q.; Wang, X.N. Effects of initial flow velocity fluctuation in event-by-event (3+1)D hydrodynamics. *Phys. Rev. C* **2012**, *86*, 024911. [CrossRef]
9. Van Hees, H.; Greco, V.; Rapp, R. Heavy-quark probes of the quark-gluon plasma at RHIC. *Phys. Rev. C* **2006**, *73*, 034913. [CrossRef]
10. Yang, M.; Zheng, S.; Tong, B.; Zhao, J.; Ouyang, W.; Zhou, K.; Chen, B. Bottom energy loss and nonprompt J/ψ production in relativistic heavy ion collisions. *Phys. Rev. C* **2023**, *107*, 054917. [CrossRef]
11. Xing, W.J.; Li, S.Q.; Cao, S.; Qin, G.Y. Bottom quark dynamics from nonprompt D0 and J/ψ production in Pb+Pb collisions at $\sqrt{s_{NN}}$ = 5.02 TeV. *Phys. Rev. C* **2024**, *110*, 024903. [CrossRef]
12. Zhao, J.; Aichelin, J.; Gossiaux, P.B.; Beraudo, A.; Cao, S.; Fan, W.; He, M.; Minissale, V.; Song, T.; Vitev, I.; et al. Hadronization of heavy quarks. *Phys. Rev. C* **2024**, *109*, 054912. [CrossRef]
13. Zhao, S.; He, M. Statistical production of Bc mesons in heavy-ion collisions at the LHC energy. *Phys. Lett. B* **2025**, *861*, 139283. [CrossRef]
14. Zhao, J.; Zhou, K.; Chen, S.; Zhuang, P. Heavy flavors under extreme conditions in high energy nuclear collisions. *Prog. Part. Nucl. Phys.* **2020**, *114*, 103801. [CrossRef]
15. Blaizot, J.P.; Escobedo, M.A. Quantum and classical dynamics of heavy quarks in a quark-gluon plasma. *J. High Energy Phys.* **2018**, *6*, 034. [CrossRef]
16. Hagedorn, R.; Redlich, K. Statistical Thermodynamics in Relativistic Particle and Ion Physics: Canonical or Grand Canonical? *Z. Phys. C Part. Fields* **1985**, *27*, 541. [CrossRef]
17. Hamieh, S.; Redlich, K.; Tounsi, A. Canonical description of strangeness enhancement from p-A to Pb Pb collisions. *Phys. Lett. B* **2000**, *486*, 61–66. [CrossRef]
18. Liu, Y.; Ko, C.M.; Song, T. Hot medium effects on J/ψ production in $p + Pb$ collisions at $\sqrt{s_{NN}} = 5.02$ TeV. *Phys. Lett. B* **2014**, *728*, 437–442. [CrossRef]
19. Andronic, A.; Braun-Munzinger, P.; Redlich, K.; Stachel, J. Decoding the phase structure of QCD via particle production at high energy. *Nature* **2018**, *561*, 321–330. [CrossRef]
20. Chen, Y.; He, M. Charged-particle multiplicity dependence of charm-baryon-to-meson ratio in high-energy proton-proton collisions. *Phys. Lett. B* **2021**, *815*, 136144. [CrossRef]
21. Bai, X.; Li, G.; Zhang, Y.; Situ, Q.; Chen, X. Data-driven analysis of the beauty hadron production in pp collisions at the LHC with Bayesian unfolding. *J. High Energy Phys.* **2024**, *11*, 018. [CrossRef]
22. Cao, S.; Qin, G.Y.; Bass, S.A. Energy loss, hadronization and hadronic interactions of heavy flavors in relativistic heavy-ion collisions. *Phys. Rev. C* **2015**, *92*, 024907. [CrossRef]
23. Chen, B.; Wen, L.; Liu, Y. Bc+ formation from random charm and anti-bottom quarks in the quark-gluon plasma. *Phys. Lett. B* **2022**, *834*, 137448. [CrossRef]
24. Chen, B.; Jiang, L.; Liu, X.H.; Liu, Y.; Zhao, J. X(3872) production in relativistic heavy-ion collisions. *Phys. Rev. C* **2022**, *105*, 054901. [CrossRef]
25. Xu, Y.; Bernhard, J.E.; Bass, S.A.; Nahrgang, M.; Cao, S. Data-driven analysis for the temperature and momentum dependence of the heavy-quark diffusion coefficient in relativistic heavy-ion collisions. *Phys. Rev. C* **2018**, *97*, 014907. [CrossRef]
26. Schenke, B.; Jeon, S.; Gale, C. Elliptic and triangular flow in event-by-event (3+1)D viscous hydrodynamics. *Phys. Rev. Lett.* **2011**, *106*, 042301. [CrossRef]
27. Schenke, B.; Jeon, S.; Gale, C. (3+1)D hydrodynamic simulation of relativistic heavy-ion collisions. *Phys. Rev. C* **2010**, *82*, 014903. [CrossRef]

28. Shen, C.; Qiu, Z.; Song, H.; Bernhard, J.; Bass, S.; Heinz, U. The iEBE-VISHNU code package for relativistic heavy-ion collisions. *Comput. Phys. Commun.* **2016**, *199*, 61–85. [CrossRef]
29. Zhu, X.; Xu, N.; Zhuang, P. The Effect of partonic wind on charm quark correlations in high-energy nuclear collisions. *Phys. Rev. Lett.* **2008**, *100*, 152301. [CrossRef]
30. Greco, V.; Ko, C.M.; Rapp, R. Quark coalescence for charmed mesons in ultrarelativistic heavy ion collisions. *Phys. Lett. B* **2004**, *595*, 202–208. [CrossRef]
31. Song, T.; Berrehrah, H. Hadronization time of heavy quarks in nuclear matter. *Phys. Rev. C* **2016**, *94*, 034901. [CrossRef]
32. Shi, S.; Zhao, J.; Zhuang, P. Heavy flavor dissociation in framework of multi-body Dirac equations. *Chin. Phys. C* **2020**, *44*, 084101. [CrossRef]
33. Zhao, W.; Ko, C.M.; Liu, Y.X.; Qin, G.Y.; Song, H. Probing the Partonic Degrees of Freedom in High-Multiplicity $p-Pb$ collisions at $\sqrt{s_{NN}}$ = 5.02 TeV. *Phys. Rev. Lett.* **2020**, *125*, 072301. [CrossRef]
34. Zhu, X.l.; Zhuang, P.f.; Xu, N. J/psi transport in QGP and p(t) distribution at SPS and RHIC. *Phys. Lett. B* **2005**, *607*, 107–114. [CrossRef]
35. Chen, B.; Hu, M.; Zhang, H.; Zhao, J. Probe the tilted Quark-Gluon Plasma with charmonium directed flow. *Phys. Lett. B* **2020**, *802*, 135271. [CrossRef]
36. Chen, S.; He, M. Heavy quarkonium dissociation by thermal gluons at next-to-leading order in the Quark–Gluon Plasma. *Phys. Lett. B* **2018**, *786*, 260–267. [CrossRef]
37. Zhao, X.; Rapp, R. Charmonium in Medium: From Correlators to Experiment. *Phys. Rev. C* **2010**, *82*, 064905. [CrossRef]
38. Andronic, A.; Gossiaux, P.B.; Petreczky, P.; Rapp, R.; Strickland, M.; Blaizot, J.P.; Brambilla, N.; Braun-Munzinger, P.; Chen, B.; Delorme, S.; et al. Comparative study of quarkonium transport in hot QCD matter. *Eur. Phys. J. A* **2024**, *60*, 88. [CrossRef]
39. Liu, Y.; Qu, Z.; Xu, N.; Zhuang, P. Rapidity Dependence of J/psi Production at RHIC and LHC. *J. Phys. G* **2010**, *37*, 075110. [CrossRef]
40. Sjöstrand, T.; Ask, S.; Christiansen, J.R.; Corke, R.; Desai, N.; Ilten, P.; Mrenna, S.; Prestel, S.; Rasmussen, C.O.; Skands, P.Z. An introduction to PYTHIA 8.2. *Comput. Phys. Commun.* **2015**, *191*, 159–177. [CrossRef]
41. Yan, L.; Zhuang, P.; Xu, N. Competition between J/psi suppression and regeneration in quark-gluon plasma. *Phys. Rev. Lett.* **2006**, *97*, 232301. [CrossRef] [PubMed]
42. Chen, B. Thermal production of charmonia in Pb-Pb collisions at $\sqrt{s_{NN}} = 5.02$ TeV. *Chin. Phys. C* **2019**, *43*, 124101. [CrossRef]
43. Zhang, Y.f. Overview of charm production at RHIC. *J. Phys. G* **2008**, *35*, 104022. [CrossRef]
44. Song, T.; Ko, C.M.; Lee, S.H. Quarkonium formation time in relativistic heavy-ion collisions. *Phys. Rev. C* **2015**, *91*, 044909. [CrossRef]
45. Acharya, S.; ALICE Collaboration. Measurements of inclusive J/ψ production at midrapidity and forward rapidity in Pb–Pb collisions at sNN = 5.02 TeV. *Phys. Lett. B* **2024**, *849*, 138451. [CrossRef]
46. Adare, A.; PHENIX Collaboration. J/ψ Production vs Centrality, Transverse Momentum, and Rapidity in Au+Au Collisions at $\sqrt{s_{NN}} = 200$ GeV. *Phys. Rev. Lett.* **2007**, *98*, 232301. [CrossRef]